Progr Colloid Polym Sci (2006) 133: 131–141
DOI 10.1007/2882_072

Published online: 6 May 2006

Paulo A. R. Pires
Omar A. El Seoud

Benzyl (3-Acylaminopropyl) Dimethylammonium Chloride Surfactants: Structure and Some Properties of the Micellar Aggregates

Paulo A. R. Pires · Omar A. El Seoud (✉)
Instituto de Química, Universidade de São Paulo, C.P. 26077, 05513-970 São Paulo, Brazil
e-mail: elseoud@iq.usp.br

Abstract The title cationic surfactants were synthesized by the scheme in Fig. 1, where RCO_2H refers to decanoic, dodecanoic, tetradecanoic and hexadecanoic acid, respectively. In aqueous solution, the micelle/water interface may be located at the quaternary ammonium ion or at the amide group. The following pieces of evidence indicate that the interface lies at the latter site: theoretically calculated aggregation numbers and those determined by static light scattering; dependence on surfactant concentration, below and above the critical micelle concentration, cmc, of both the IR frequency of amide I band and ^{1}H NMR chemical shifts of the discrete surfactant protons. Solution conductance and calorimetric titration have been employed to study the aggregation of these surfactants in water at 25 °C. Increasing the length of R resulted in a decrease of the cmc and the degree of counter–ion dissociation, α_{mic}. Gibbs free energies of micelle formation were calculated and divided into contributions from the methylene groups of the hydrophobic tail, and the terminal methyl plus head-group. The former are similar to those of other surfactants, whereas the latter are more negative, i.e., the transfer of the head-group from bulk water to the micelle is more favorable. This is attributed to direct or water-mediated H-bonding of the micellized surfactant molecules, via the amide group, in agreement with the IR data presented.

Keywords Aggregation numbers · Benzyl (3-acylaminopropyl) dimethylammonium chloride surfactants · Cationic surfactants · Counter–ion dissociation · Critical micelle concentration

Introduction

The structural variables of surfactants include the length of the hydrophobic tail, the nature of the counter–ion, and the structure/charge of the head-group. Although many important applications of surfactant solutions, e.g., solubilization, emulsion formation and catalysis reflect substrate–head-group interactions, the latter structural variable has been much less studied than the former ones [1–7]. Cationic surfactants are amenable to this line of study because the structure of their head-group can be changed while maintaining constant the nature of the head-ion, e.g. quaternary ammonium. Work has been carried out on surfactants whose general structure is given by: $RN^+R'R''R'''\ X^-$, where X^- = halide ion; R = octyl to octadecyl; R′, R″, and R‴ generally represent iden-

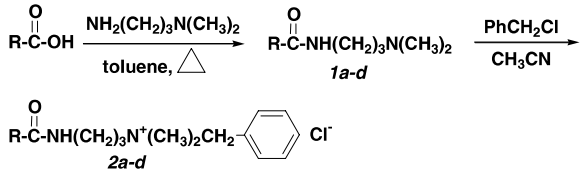

Fig. 1

tical alkyl groups, e.g., trimethyl. A number of studies have employed R′ and R″ = methyl and R‴ = alkyl, benzyl or alkylphenyl group [1–3, 8–11]. One of the alkyl groups of the head-ion may carry functionality, e.g., the 2-hydoxyethyl group. Interestingly, the effects of this group on the micellar parameters are not significantly different from those of an ethyl group [12–16]. Surfactants that carry the amide group may, in principle, form direct or water-mediated inter-molecular hydrogen-bonds, akin to those formed by *N*-alkylamides, and polypeptides [17–19]. Additionally, surfactants that carry the amide group and a (negative) charge, separated by a "spacer" have some interesting interfacial properties, due to the simultaneous presence of both moieties [20]. We were interested, therefore, in investigating how a similar structural feature (amide group and a positive charge) bears on solution properties of surfactants.

Recently, we studied the micellar properties of $RCONH(CH_2)_2N^+(CH_3)_3Cl^-$, and $RCONH(CH_2)_2N^+(CH_3)_2CH_2C_6H_5Cl^-$, where RCO = C_{10}, C_{12}, C_{14} and C_{16}, respectively. Gibbs free energies of micelle formation were found to be more favorable than those of structurally similar cationic surfactants that do not carry the amide group. This was attributed to direct or water-mediated hydrogen-bonding between the surfactant molecules in the aggregate [21–26]. We report here on the synthesis of the following series: $RCONH(CH_2)_3N^+(CH_3)_2CH_2C_6H_5Cl^-$, where RCO = C_{10}, C_{10}APrBzMe$_2$Cl; C_{12}, C_{12}APrBzMe$_2$Cl; C_{14}, C_{14}APrBzMe$_2$Cl; and C_{16}, C_{16}APrBzMe$_2$Cl; (A), (Pr) and (Bz) stand for ($-NH(CH_2)_3N^+$), *n*-C_3H_6 and the benzyl group, respectively. IR data of the amide I band of C_{10}APrBzMe$_2$Cl and that of a short-chain, i.e., non-aggregated analogue indicated that the amide group in the micelle is hydrated, i.e., present in the interfacial region. ^{1}H NMR data of the discrete surfactant protons, below and above the cmc, indicated that the benzyl group "folds back" toward the aggregate interior. Gibbs free energies of micellization of the surfactants studied are more favorable than those of $RN^+(CH_3)_2CH_2C_6H_5Cl^-$, RBzMe$_2$Cl, due to the above-mentioned hydrogen-bonding.

Experimental

Materials

The chemicals were purchased from Acros or Merck, and were purified by standard procedures [27]. The series RBzMe$_2$Cl was available from a previous study [25].

Apparatus

Melting points were determined with Electrothermal IA 6304 apparatus. We used Shimadzu model GC 17A-2 gas chromatograph equipped with FID detector and Supelcowax 10 capillary column (from Supelco). FTIR spectra were recorded with a Bruker Vector 22 spectrometer. ^{1}H and ^{13}C NMR spectra were recorded with Varian Innova-300 or Bruker DRX-500 spectrometers. Elemental analyses were carried out on Perkin-Elmer model 2400 CHN apparatus in the Elemental Analyses laboratory of this Institute.

Synthesis

Chromatographically pure carboxylic acids were obtained as follows: Ethyl esters of the decanoic to hexadecanoic acids were prepared by their reaction with anhydrous ethanol (Mensalão Química, DF), in the presence of H_2SO_4 as catalyst. The esters were purified by fractional distillation under reduced pressure in a 50 cm Vigreux column. This process was repeated until the ester was chromatographically pure. The following conditions were employed in the CG analysis: Injector temperature 250 °C; FID temperature 280 °C; carrier gas N_2, 1.5 cm^3/min, split ratio 1 : 50. The column was kept at 100 °C for 8 minutes, heated at 10 °C/minute for 5 minutes, kept at 150 °C for 15 minutes, heated at 10 °C/minute for 5 minutes, then kept at 200 °C for the rest of the analysis. The retention times were 15.7, 24.7, 34.0, 41.2 minutes, for the ethyl esters of decanoic, dodecanoic, tetradecanoic, and hexadecanoic acid, respectively. The corresponding acids were obtained by alkaline hydrolysis in 50% aqueous methanol, followed by removal of the solvent and acidification with HCl. The carboxylic acid was separated, washed with hot water until the aqueous phase was free of Cl^-, and dried. The physical properties of the acids obtained agree with literature values [28].

Amidoamines, $RCONH(CH_2)_3N(CH_3)_2$, Compounds 1a to 1d

The following reaction was carried out under dry, oxygen-free nitrogen: to a stirred solution of the carboxylic acid (0.70 mol) in 250 mL of toluene were added, drop-wise, 88 mL (0.70 mol) of 3-*N*,*N*-dimethylamino-1-propylamine. The bath temperature was raised to 120–130 °C, and the formation of the product was followed by measuring the volume of the water produced (Dean-Stark trap), and by monitoring the disappearance of the $\nu_{C=O}$ peak of the free acid at ca. 1720 cm^{-1}; usually 16 hours were required for reaction completion. After solvent evaporation, product (**1**) was purified either by fractional distillation, **1a** and **1b**, or by recrystallization from anhydrous acetone, **1c** and **1d**. TLC analysis of each product showed a single spot.

Compound **1a**, $C_9H_{19}CONH(CH_2)_3N(CH_3)_2$.

Colorless, viscous liquid, b.p. 179.5–181.0 °C (1.5 mm Hg); yield, 74%. IR (film, NaCl plates, frequencies are reported in cm^{-1}) 3290 (n_{N-H}, secondary amide), 1645 (amide I band), 1554 (amide II band). The structures depicted below show the numbering employed for

reporting the ^{1}H, and ^{13}C NMR data, respectively, where n = total number of equivalent hydrogens (due to virtual coupling) or equivalents carbons of the chain:

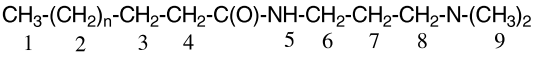

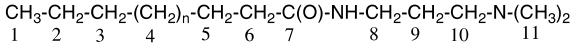

^{1}H NMR ($CDCl_3$, chemical shifts, δ and coupling constants, J, are reported in ppm and Hz, respectively): 0.88 (t, 3H, **H1**, $J_{1-2} = 7.1$), 1.27 (broad peak, 12H, **H2**), 1.61 (quintet, 2H, **H3**, $J_{2-3} = 7.3$ and $J_{3-4} = 7.5$), 2.17 (t, 2H, **H4**), 7.60 (broad singlet, 1H, **H5**), 3.28 (multiplet, 2H, **H6**, $J_{6-5} = 6.1$; $J_{6-7} = 6.4$); 1.67 (doublet of triplets, 2H, **H7**, $J_{7-8} = 6.7$); 2.38 (triplet, 3H, **H8**), 2.24 (s, 6H, **H9**).

^{13}C NMR ($CDCl_3$): 14.12 (C**1**), 22.69 (C**2**), 31.91 (C**3**), 29.34 to 29.55, (*four lines*, C**4**), 25.93 (C**5**), 36.73 (C**6**), 173.37 (C**7**), 38.59 (C**8**), 26.63 (C**9**), 58.03 (C**10**), 45.23 (C**11**).

Compound **1b**, $C_{11}H_{23}CONH(CH_2)_3N(CH_3)_2$.

White waxy solid; mp 31–33 °C, bp 208–211 °C (3.5 mm Hg); yield, 90%. IR (KBr) 3306 (n_{N-H}, secondary amide), 1641 (amide I band), 1555 (amide II band).

The ^{1}H NMR and ^{13}C NMR spectra of compounds **1b–1d** ($CDCl_3$) were found to be similar to those of **1a**, within the following limits: ^{1}H NMR (0 to ±0.005 ppm) and ^{13}C NMR (±0.03 ppm). For all compounds, the ^{13}C NMR region for C**4** showed 6 lines.

Compound **1c**, $C_{13}H_{27}CONH(CH_2)_3N(CH_3)_2$.

White waxy solid; mp 48–49 °C; bp 193–195 °C (0.5 mm Hg); yield, 60%. The IR spectra (KBr) of compounds **1c,d** are similar to that of **1b**, within the following limits: ±3 cm^{-1} for n_{N-H} and ±1 cm^{-1} for amide I and II bands.

Compound **1d**, $C_{15}H_{31}CONH(CH_2)_3N(CH_3)_2$.

White solid; mp 57–58 °C; yield, 83%.

Surfactants

The following reaction was carried out under dry, oxygen-free nitrogen: a mixture of 0.1 mol of compound **1** and 12.6 mL (0.11 mol) of benzyl chloride in 100 mL of anhydrous acetonitrile was refluxed for 8 hours. The solvent and un-reacted benzyl chloride were removed, the product was recrystallized from anhydrous acetone and dried under reduced pressure. All surfactants were hygroscopic solids, and were analyzed as (non-hygroscopic) perchlorate salts. The structures depicted below show the numbering employed for reporting the ^{1}H, and ^{13}C NMR data of the surfactant cation, respectively. Note that the (ortho) and (meta) ring protons form the AA′ and BB′ part of the aromatic ring:

For ^{1}H NMR

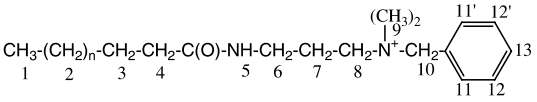

For ^{13}C NMR

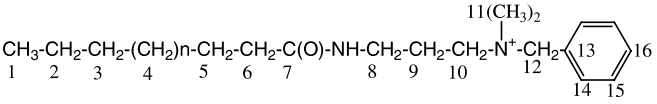

Surfactant 2a, C_{10}APrBzMe$_2$Cl**:** yield, 80%; Anal. Calcd for $C_{22}H_{39}N_2O_5Cl$: C, 59.16; H, 8.81; N, 6.28. Found: C, 58.94; H, 8.64; N, 6.35. IR (KBr), 3277 (n_{N-H}, secondary amide), 1649 (amide I band), 1555 (amide II band). ^{1}H NMR: ($CDCl_3$): 0.87 (t, 3H, **H1**, $J_{1-2} = 7.1$), 1.22 (broad peak, 12H, **H2**), 1.53 (quintet, 2H, **H3**, $J_{2-3} =$ 6.5 and $J_{3-4} = 7.2$), 2.22 (t, 2H, **H4**), 3.32 (quadruplet, 2H, **H6**, $J_{6-5} = 10.4$ and $J_{6-7} = 6.0$), 2.17 (doublet of triplets, 2H, **H7**, $J_{7-8} = 9.7$), 3.63 (t, 3H, **H8**), 3.17 (s, 6H, **H9**), 4.81 (s, 2H, **H10**); 7.61 (d, 2H, **H11**(**11′**), $J_{11-12} =$ 6.9); 7,39 (multiplet, 2H, **H12**(**12′**), $J_{12-13} = 7.2$); 7.44 (multiplet, 1H, **H13**).

^{13}C NMR ($CDCl_3$): 14.11 (C**1**), 22.63 (C**2**), 31.84 (C**3**), 29.30 to 29.52 (four lines, C**4**), 25.83 (C**5**), 36.29 (C**6**), 174.52 (C**7**), 36.16 (C**8**), 23.06 (C**9**), 62.27 (C**10**), 49.74 (C**11**); 67.33 (C**12**); 127.36 (C**13**); 133.15 (C**14**); 129.17 (C**15**); 130.66 (C**16**).

Surfactant 2b, C_{12}APrBzMe$_2$Cl**:** yield, 72%. Anal. Calcd for $C_{24}H_{43}N_2O_5Cl$: C, 60.72; H, 9.14; N, 5.90. Found: C, 60.86; H, 8.95; N, 5.83.

The spectroscopic data for this surfactant and for the others below, are similar to those of **2a**, within the following limits: IR (±2 cm^{-1}, and 4 cm^{-1} for the N – H proton, amide I and amide II band, respectively), ^{1}H NMR (0 to ±0.01 ppm for the aliphatic and aromatic protons and 0.02 ppm for the NH proton), ^{13}C NMR (±0.02 ppm).

Surfactant 2c, C_{14}APrBzMe$_2$Cl**:** yield, 69%. Anal. Calcd for $C_{26}H_{47}N_2O_5Cl$: C, 62.11; H, 9.43; N, 5.58. Found: C, 62.14; H, 9.30; N, 5.82.

Surfactant 2d, C_{16}APrBzMe$_2$Cl**:** yield, 75%. Anal. Calcd for $C_{28}H_{51}N_2O_5Cl$: C, 63.35; H, 9.69; N, 5.28. Found: C, 63.27; H, 9.40; N, 5.15.

Short-chain Analogue of Surfactants, C_4APrBzMe$_2$Cl

This compound (white solid) was synthesized according to the procedure described above, by employing butyric acid. The structure depicted below shows the numbering employed for reporting the ^{1}H NMR data of the cation:

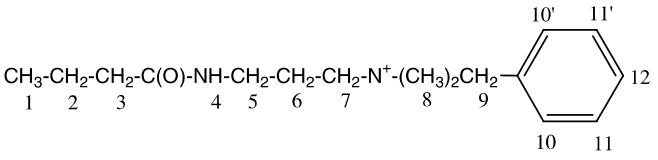

IR (KBr): 3446 (n_{N-H}, secondary amide), 1653 (amide I band), 1548 (amide II band). ^{1}H NMR ($CDCl_3$): 0.88 (t, 3H, **H1**, $J_{1-2} = 7.4$), 1.60 (sextet, 2H, **H2**, $J_{2-3} = 7.5$), 2.26 (t, 2H, **H3**), 3.36 (doublet of triplets, 2H, **H5**, $J_{4-5} = 6.0$ $J_{5-6} = 6.0$), 2.19 (quintet, 2H, **H6**, $J_{6-7} = 7.4$); 3.77 (triplet, 2H, **H7**); 3.23 (s, 9H, **H8**), 4.89 (s, 2H, **H9**); 7.64 (doublet of triplets, 2H, **H10(10′)**, $J_{10-11} = 7.0$ and $J_{10-12} = 1.3$); 7,43 (multiplet, 2H, **H11(11′)**, $J_{11-12} = 7.6$); 7.48 (multiplet, 1H, **H12**).

Measurements of Properties of Micellar Solutions

Glass double-distilled, de-ionized water was used throughout. Before use, all glassware was soaked in 0.001M EDTA solution and thoroughly washed with water. Each surfactant was weighted, dried under reduced pressure, over P_4O_{10} until constant weight before making up the solution.

Solution Conductivity

Conductivity measurements were recorded for RAPrBzMe_2Cl or RBzMe_2Cl at 25 °C with a PC-interfaced Fisher model Accumet 50 ion-meter, provided with a DM-C1 micro-conductivity cell (Digimed, São Paulo) and a Schott model Titronic T200 programmed burette. Home-developed software was employed for addition of the surfactant solution and data acquisition. Plots of conductivity versus the total surfactant concentration, $[\mathrm{Surf}]_t$, gave two straight lines intersecting at the cmc. The following equation was employed in order to obtain a more accurate cmc [29]:

$$\kappa([\mathrm{Surf}]_t) = \kappa(0) + S_1[\mathrm{Surf}]_t + \mathrm{d}x(S_2 - S_1)\ln\left(\frac{1 + \mathrm{e}^{([\mathrm{Surf}]_t - \mathrm{cmc})/\mathrm{d}x}}{1 + \mathrm{e}^{-\mathrm{cmc}/\mathrm{d}x}}\right), \quad (1)$$

where $\kappa([\mathrm{Surf}]_t)$, $\kappa(0)$, S_1, S_2, and dx are the conductivity of the solution (i.e., at $[\mathrm{Surf}]_t$) and at infinite dilution, the slopes of the pre- and post-micellar regions of conductivity versus [surfactant] plot, and the width of the cmc transition (d$x \approx 10\%$ of the cmc), respectively.

The degree of dissociation of the surfactant counter–ion, α_{mic}, was calculated from conductance data by use of two equations, that of Frahm [30]:

$$\alpha_{mic} = (S_2/S_1), \quad (2)$$

where S_1 and S_2 are the slopes of the pre- and post-cmc regions of conductivity versus [surfactant] plot. The second equation is that of Evans [31]:

$$1000S_2 = \frac{\alpha_{mic}^2}{(N_{agg})^{-2/3}}\left(1000S_1 - \Lambda_{Cl^-}\right) + \alpha_{mic}\Lambda_{Cl^-}, \quad (3)$$

where Λ_{Cl^-} refers to the equivalent conductance of the surfactant counter–ion at infinite dilution and N_{agg} is the micellar aggregation number; the other symbols have their usual meaning.

FTIR Measurements

The cmc of C_{10}APrBzMe_2Cl in D_2O was determined by FTIR, by employing the above-mentioned spectrometer, and a 0.025 mm path-length CaF_2 cell (Wilmad Glass). The spectrometer sample compartment was flushed with dry nitrogen. The frequency of amide I band was measured as function of [surfactant], at 0.5 cm^{-1} digital resolution. The background spectrum of pure D_2O was subtracted from the spectrum of the sample.

Static Light Scattering (SLS)

Static light scattering was recorded at 25 ± 0.1 °C with Malvern 4700 system. The surfactant solutions contained 0.1 mol L^{-1} NaCl, and were filtered through 0.22 μm cellulose acetate membranes. All measurements were recorded at 90° scattering angle, by employing a home-developed software for scattering data acquisition. Solution refractive index increment was measured with Wyatt Optilab 903 interferometric differential refractometer, operating at 633 nm.

The micellar weight-averaged molar mass, M_w, was calculated by [3]:

$$K([\mathrm{Surf}]_t - \mathrm{cmc})/\Delta R_{90} = 1/M_w + 2B([\mathrm{Surf}]_t - \mathrm{cmc}), \quad (4)$$

where ΔR_{90} is the Rayleigh ratio of micellized surfactant, $\Delta R_{90} = R_{90}$ (surfactant solution) – R_{90} (surfactant solution at cmc), $[\mathrm{Surf}]_t$ and cmc are expressed in g/L, B is the second virial coefficient, and K is the optical constant, expressed by:

$$K = \frac{2\pi^2 n_0^2 (\mathrm{d}n/\mathrm{d}[\mathrm{Surf}]_t)^2}{N_{AV}\lambda^4}, \quad (5)$$

where n_o is the refractive index of the solution at the cmc, $\mathrm{d}n/\mathrm{d}[\mathrm{Surf}]_t$ is the solution refractive index increment, N_{AV} is the Avogrado's number and λ is the wave length of the laser light in vacuum. N_{agg} is obtained by dividing M_w by the molecular weight of the monomer.

Titration Calorimetry

The experiments were carried out at 25 °C. Enthalpies of micellization, $\Delta H^{\circ}_{\mathrm{mic}}$, were measured with Thermometric AB 2277 TAM Thermal Activity Monitor system. Under constant stirring, 10 to 40 μL aliquots of the concentrated surfactant solution ([surfactant] $\approx 20 \times$ cmc), were added to 2 mL of water in the sample cell. Each injection of the titrant solution resulted in a peak, whose corresponding area was calculated, then employed in plotting the calorimetric titration curve of the heat of dilution, H_{dil}, versus [surfactant]. The cmc may be calculated from the resulting sigmoidal plot. One problem with this calculation is the small number of points registered in the cmc region, a consequence of the abrupt rise of the enthalpy as a function of [surfactant]. To improve the precision of the cmc calculated, we have fitted Eq. 6 to the heats of dilution versus [surfactant] curves [32]:

$$H_{\mathrm{dil}} = \frac{a_1 \cdot [\mathrm{Surf}]_t + a_2}{1 + \mathrm{e}^{\frac{([\mathrm{Surf}]_t - a3)}{\mathrm{d}x}}} + a_4 \cdot [\mathrm{Surf}]_t + a_5 \,, \tag{6}$$

where a_1 to a_5 are fitting parameters and the other symbols have their usual meaning. For all surfactants studied the best fit was obtained by taking, as initial guesses, a_1, a_4, and $a_5 =$ unity, $a_2 = \Delta H^{\circ}_{\mathrm{mic}}$, obtained graphically from the calorimetric titration curve, $a_3 =$ conductivity-based cmc, and $\mathrm{d}x = 10\%$ of the cmc. In all computations, convergence was achieved, and iteration-based a_2 and a_3 were in agreement with the values determined experimentally. The cmc values reported were taken as the maximum, or minimum of the first derivative of Eq. 6.

Calculation of the Thermodynamic Parameters of Micellization

Gibbs free energy of micellization, $\Delta G^{\circ}_{\mathrm{mic}}$, was calculated by the use of Eq. 7 (based on the Mass-Action Law):

$$\Delta G^{\circ}_{\mathrm{mic}} = (2 - \alpha_{\mathrm{mic}}) \mathrm{R}\, T\, \mathrm{Ln}(\chi_{\mathrm{cmc}}) \,, \tag{7}$$

where χ_{cmc} is the cmc expressed on mole fraction scale, R is the universal gas constant and T is the temperature, in K. From calorimetry-based $\Delta H^{\circ}_{\mathrm{mic}}$ and Gibbs free energy equation, the entropy of micellization, $\Delta S^{\circ}_{\mathrm{mic}}$ may be readily calculated by Eq. 8:

$$\Delta G^{\circ}_{\mathrm{mic}} = \Delta H^{\circ}_{\mathrm{mic}} - T \Delta S^{\circ}_{\mathrm{mic}} \,. \tag{8}$$

Results and Discussion

Site of the Micelle-water Interface

Values of cmc and α_{mic} may be readily calculated from conductance measurements. Data treatment according to Evans equation requires knowledge of the micelle aggregation number, N_{agg}. A problem arises, however, with surfactants that carry the amide group, because of the uncertainty regarding the (average) site of the micellar interface. This may be at the amide group, or at the quaternary ammonium ion, $\mathrm{R}\underline{\mathrm{CO-NH}}(\mathrm{CH_2})_3\underline{\mathrm{N^+}}(\mathrm{CH_3})_2\mathrm{BzCl^-}$, respectively. Additionally, the conformation of the benzyl group with respect to the interface is unknown. We start our discussion, therefore, by addressing these questions. Figure 2 shows some limiting possibilities for the micelle: Structures 1 and 2 show that the interface lies at the quaternary ammonium ion, i.e., the amide group is present in a relatively hydrophobic medium, some 3 methylene groups away from the interface. The same structures show two possible conformations for the benzyl group, perpendicular and parallel to the interface, respectively. Alternatively, the interface may lie at the amide group, as depicted in structures 2 to 5. Because of the flexibility of the $\mathrm{NH(CH_2)_3N^+(CH_3)_2-CH_2C_6H_5}$ "tether", the benzyl group may assume different conformations with respect to the interface, perpendicular, parallel, or may "fold back" toward the micellar interior.

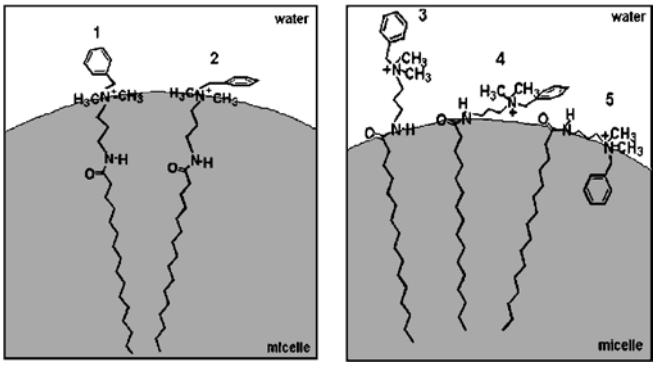

Fig. 2 Possible sites for the micelle/water interface and conformations of surfactant polar group with respect to the aggregate surface

These questions have been solved by employing theoretical calculations, SLS, FTIR and ^{1}H NMR, respectively. Values of N_{agg} may be calculated by dividing the volume of the micelle by that of the monomer. The former was calculated by taking R1 or R2 as the micellar radius (see Fig. 3), by assuming that the aggregate is spherical and that monomers inside the micelle are present in stretched, all-trans conformation. The geometry of the monomer was optimized by employing the PM3 semi-empirical method.

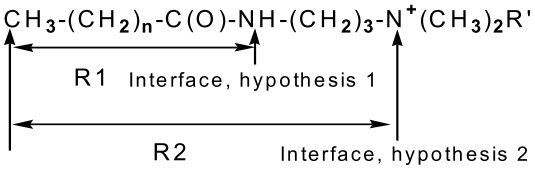

Fig. 3 Possible Sites for the micelle/water interface

Table 1 Use of different technique to study the dependence on surfactant structure of the critical micelle concentrations, cmc, degree of counter–ion dissociation, α_{mic}, micellar aggregation number, N_{agg}, Gibbs free energy of micelle formation, ΔG°_{mic}, enthalpy, ΔH°_{mic}, and the entropic term, $T\Delta S^{\circ}_{mic}$ [a]

Surfactant	N_{agg} [b]	$10^3 \times$ Cmc, mol/L, conductance	$10^3 \times$ Cmc, mol/L, calorimetry	α_{mic} [c]	ΔG°_{mic} [d] (kJ mol^{-1})	ΔH°_{mic} (kJ mol^{-1})	$T\Delta S^{\circ}_{mic}$ [d] (kJ mol^{-1})
$C_{10}APrBzMe_2Cl$	43; 48	21.0	21.6	0.27 (0.34)	−33.8, −33.7	0.6	34.4, 34.3
$C_{12}APrBzMe_2Cl$	61; 89	5.00	6.1	0.23 (0.30)	−40.9, −40.7	−2.1	38.8, 38.6
$C_{14}APrBzMe_2Cl$	82; 114	1.35	1.31	0.21 (0.42)	−47.1, −47.3	−5.2	41.9, 42.1
$C_{16}APrBzMe_2Cl$	107; 167; (101)	0.30	0.39	0.19 (0.48)	−54.4, −53.2	−7.2	47.2, 46.0
$C_{10}AEtBzMe_2Cl$ [e]	43	24.0	24.6	0.28 (0.35)	−32.7, −32.9	0.6	33.3, 33.5
$C_{12}AEtBzMe_2Cl$ [e]	61	5.9	6.0	0.23 (0.35)	−40.1, −40.0	−2.3	37.8, 37.7
$C_{14}AEtBzMe_2Cl$ [e]	82	1.41	1.33	0.22 (0.38)	−46.3, −46.9	−6.0	40.3, 40.9
$C_{16}AEtBzMe_2Cl$ [e]	107	0.35	0.37	0.19 (0.38)	−53.0, −53.4	−8.8	44.2, 44.6
$C_{10}BzMe_2Cl$	43	37.3	37.0 [f]	0.32 (0.43)	−30.5, −30.4	4.0 [f]	34.5, 34.4
$C_{12}BzMe_2Cl$	61	8.09	7.93 [f]	0.24 (0.38)	−38.3, −38.6	2.1 [f]	40.4, 40.7
$C_{14}BzMe_2Cl$	82	1.94	2.41 [f]	0.23 (0.46)	−45.0, −44.1	−1.7 [f]	43.3, 42.4
$C_{16}BzMe_2Cl$	107, 90 [g]	0.39	0.33 [f]	0.22 (0.40)	−52.3, −53.1	−4.6 [f]	47.7, 48.5

[a] All measurements were carried out at 25 °C. The uncertainty limits of cmc, determined by *each technique* were found to be $\leq 0.5\%$. The reasons for the observed (small but persistent) dependence of cmc on the technique employed have been discussed elsewhere. For example, Mukerjee and Mysels [66] have compiled 54 cmcs for sodium dodecyl sulfate and cetyltrimethylammonium bromide (measurements at 25 °C) , differing, for the same technique, by 100% and 22%, respectively.

[b] For $RAPrBzMe_2Cl$ the values of N_{agg} are those calculated by using molecular geometry, and those derived from SLS measurements (in the presence of 0.1 M NaCl). The third N_{agg} reported for $C_{16}APrBzMe_2Cl$ (101) is that in the absence of additional electrolyte, NaCl. For $RAEtBzMe_2Cl$ and $RBzMe_2Cl$ the values of N_{agg} were calculated by using molecular geometry

[c] Values of α_{mic} are listed in following order: calculated by Evan's method, and by Frahm's method (value within parentheses).

[d] Values of ΔG°_{mic} and $T\Delta S^{\circ}_{mic}$ are based on α_{mic} calculated by Evan's method, and conductance-based and calorimetry-based cmc, respectively

[e] Cmc values were taken from [26], α_{mic} and ΔG°_{mic} were taken from [22], and ΔH°_{mic} were taken from [25]

[f] Cmc by calorimetry and ΔH°_{mic} taken from [25]

[g] N_{agg}, determined by fluorescence, taken from [11]

The following N_{agg} were calculated: 43, 61, 82, 107 (interface at R1) and 83, 108, 136, 167 (interface at R2), for RCO = C_{10}, C_{12}, C_{14}, and C_{16}, respectively. The latter values were considered too high and may, therefore, be rejected. SLS-based N_{agg} are listed in the second column of Table 1. They are higher than those based on molecular volume calculations because the "solvent" employed was 0.1 mol/L NaCl, in order to screen inter-micellar interactions. The presence of an additional electrolyte (with the same counter–ion) leads to micellar growth, i.e., higher N_{agg} [1–3]. The cmc of $C_{16}APrBzMe_2Cl$ is, however, small so that electrostatic interactions may be safely ignored. As seen in column 2 of Table 1, the aggregation number obtained in the absence of NaCl, 101, is in good agreement with volume-based N_{agg}.

IR data of amide I bands of $C_4APrBzMe_2Cl$ and $C_{10}APrBzMe_2Cl$ (in D_2O) support the previous conclusion about the site of the micelle/water interface. As previously shown for amides and polypeptides, this band is a sensitive probe for the state of hydration of the C = O group [17–19, 33, 34]. Consider *N*-methylacetamide, because it has been extensively employed as a model compound. In dilute aqueous solutions, the carbonyl group is hydrated, resulting in $\nu_{C=O}$ at ca. 1626 cm^{-1} [35–39]. Solubilization of this amide in binary solvent mixtures whose polarities mimic that of interfacial water, e.g., aqueous alcohols results in a blue shift of $\nu_{C=O}$, directly proportional to the concentration of the organic component of the binary mixture [40, 41]. This has been attributed to dehydration of the CO group, due to partial substitution of CO-water hydrogen-bonds with amide-amide ones [9a,18c]. Further loss of hydrogen-bonding leads to much higher $\nu_{C=O}$, e.g., 1697 cm^{-1}, 1683 cm^{-1} and 1667 cm^{-1} in hexane, THF and DMSO, respectively [35–39].

A similar behavior has been observed for amide I band of $C_4APrBzMe_2Cl$, a short-chain, i.e., non-aggregated model for the surfactants. Thus the following results were observed for 0.05 mol/L solutions ($\nu_{C=O}$ in cm^{-1}, solvent employed): 1663, DMSO; 1620, D_2O; 1622, 45 mol/L D_2O in CH_3OD; 1625, 30 mol/L D_2O in CH_3OD. Comparison of the results in pure D_2O and in D_2O/CH_3OD clearly shows the blue shift caused by partial loss of

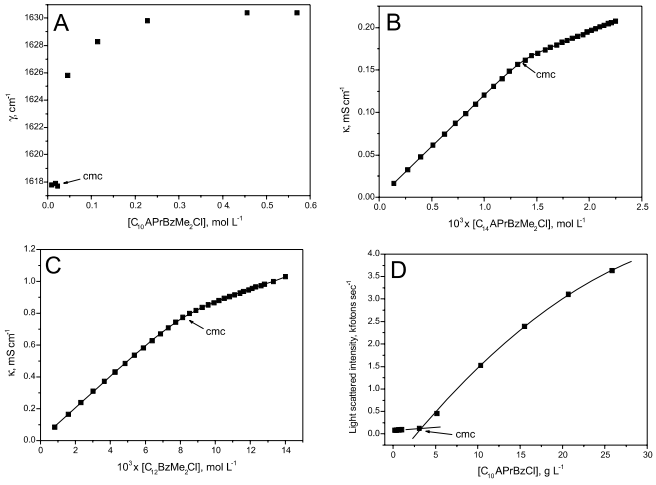

Fig. 4 Dependence of solution properties on surfactant concentration, at 25 °C: **A** $\nu_{C=O}$ of amide I band; **B** and **C** solution conductance; **D** intensity of light scattering. In **B** and **C** the *points* are experimental and the *lines* were calculated by using Eq. 3. The light scattering experiment was carried out in the presence of 0.1 mol/L NaCl, see Experimental

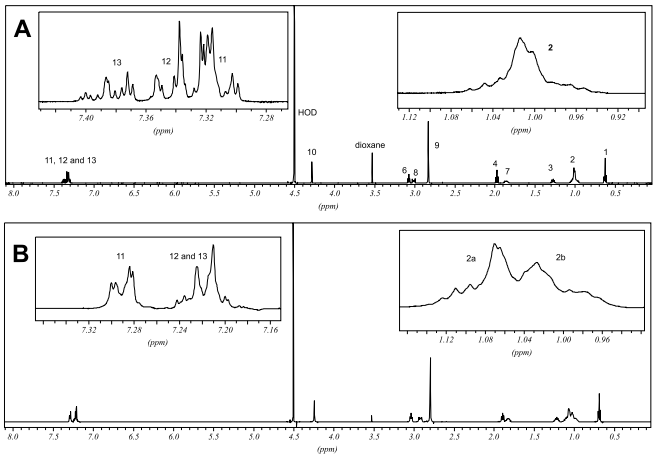

Fig. 5 Dependence of the ^{1}H NMR spectrum of $C_{12}APrBzMe_2Cl$, at 500.13 MHz, on surfactant concentration, at 6.0×10^{-3} mol L^{-1} (**A** below cmc), and 2.0×10^{-2} mol L^{-1} (**B** above cmc). See Experimental for proton designation. The spectra of the aromatic protons, below and above the cmc, may be reproduced by simulation (MestRe-C program package, version 4.5.9.1, Mestrelab Research, Santiago de Compostela, Spain). The parameters employed were: $J_{ortho} = 7.5$ Hz; $J_{meta} = 0.8$ Hz and $J_{para} = 0.5$ Hz, and the following δ (in ppm, below and above the cmc, respectively): H11 = 7.307, 7.286; H12 = 7.330, 7.172; H13 = 7.382 and 7.123

hydrogen-bonding to water, due to addition of CH_3OD. That is, the response of $\nu_{C=O}$ of $C_4APrBzMe_2Cl$ to changes in hydrogen-bonding is similar to that of *N*-methylacetamide.

At [surfactant] < cmc, the frequency of amide I band of $C_{10}APrBzMe_2Cl$ in D_2O is constant at ca. 1618 cm^{-1}, increasing rapidly to 1625 cm^{-1} just after the cmc, then levels off at 1630 cm^{-1}, at [surfactant] ≥ 0.4 mol L^{-1}, see Fig. 4A. The first frequency indicates that the monomer amide group is hydrated, akin to *N*-methylacetamide or $C_4APrBzMe_2Cl$. Above the cmc, $\nu_{C=O}$ observed, 1630 cm^{-1}, is close to that of self-associated *N*-methylacetamide. This indicates dehydration and hydrogen-bonding between molecules of $RAPrBzMe_2Cl$ in the aggregate. The relative strength of this bonding may be judged by comparing $\Delta\nu$ (= $\nu_{C=O}$ after cmc – $\nu_{C=O}$ before cmc) for $C_{10}APrBzMe_2Cl$ (12 cm^{-1}) with that of the (strongly hydrated) carboxylate head-group of sodium nonanoate or decanoate, ≤ 3 cm^{-1} [42]. Comparison of the limiting $\nu_{C=O}$ of micellized $C_{10}APrBzMe_2Cl$ with that of *N*-methylacetamide in DMSO and of $C_4APrBzMe_2Cl$ in aqueous alcohols, vide supra, shows that this group is appreciably hydrated in the aggregate, i.e., is not present in the micellar interior, as depicted by structures 1 and 2 of Fig. 2; these, therefore, may be safely rejected.

A decision regarding the conformation of the head-group may be reached by examining the dependence of δ (^{1}H NMR), and line shape on [surfactant], below and above the cmc, as shown in Fig. 5 for $C_{12}APrBzMe_2Cl$ (see Experimental for proton designation). Thus aggregation resulted in a splitting of the broad peak of H2, and an inversion of the order of δ of the aromatic ring protons, being $\delta_{H13} > \delta_{H12(12')} > \delta_{H11(11')}$ and $\delta_{H11(11')} > \delta_{H12(12')} > \delta_{H13}$, at [surfactant] below and above the cmc, respectively. This behavior has been observed for all surfactants studied (^{1}H NMR spectra not shown). Consider first the aliphatic H2 protons. Although this peak is usually broad due to virtual coupling, no splitting has been observed as a result of micellization of other ionic surfactants, e.g., sodium dodecyl sulfate or dodecyl-trimethylammonium chloride [43]. The results of $C_{12}APrBzMe_2Cl$ raise the following question: Does peak splitting of the aliphatic hydrogens occur with other surfactants that carry an aromatic head-group? Figure 6 shows that this is not necessarily the case, since there are no noticeable differences between the spectra of dodecylpyridinium chloride below, and above the cmc, except for small changes in line width and δ of the discrete groups. The preceding results point out to the following picture: the heterocyclic ring of dodecylpyridinium chloride lies perpendicular to the micellar interface, so that there is no diamagnetic deshielding/shielding of segments of the hydrophobic tail by (ring current effect of) the pyridinium ring [9]. A different behavior may be observed, however, when the surfactant carries anisotropic head-group, *whose movement is not restricted in the micelle*, e.g., the benzyl group. The flexibility of the tether allows the benzyl group of $RAPrBzMe_2Cl$ to fold back toward the micellar interior, causing the observed splitting

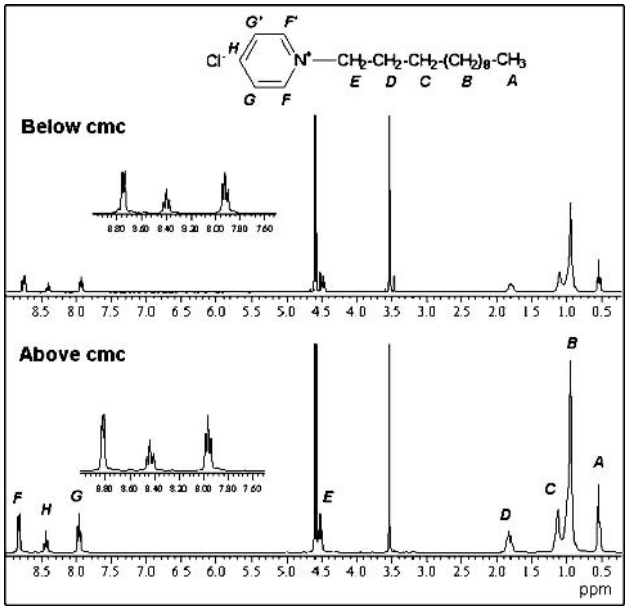

Fig. 6 Dependence of the ^{1}H NMR spectrum (300 MHz) of dodecylpyridinium chloride in D_2O on [surfactant] below (0.005 mol/L) and above (0.08 mol/L) the cmc. The singlet at 3.53 ppm is that of dioxane, employed as an internal reference

of the main CH_2 peak [24, 44]. The dependence of δ of the aromatic protons on [surfactant] is another evidence for folding back of the benzyl moiety. Below cmc the order is $\delta_{H13} > \delta_{H12(12')} > \delta_{H11(11')}$. Above the cmc, the peaks of H_{13} and $H_{12(12')}$ move up-field relative to $H_{11(11')}$ because they are transferred, on micellization, from an aqueous pseudo-phase to a less polar environment, the micelle [44].

In summary, N_{agg} calculated and those determined by SLS (in particular that of $C_{16}APrBzMe_2Cl$ in the absence of NaCl) and the dependence of $\nu_{C=O}$ on [surfactant] show that the amide head-groups in the micelles are hydrated and hydrogen-bonded, either directly or via water molecules. ^{1}H NMR chemical shifts of both aromatic and aliphatic protons show that there is interaction between the former moiety and a few of the (CH_2) groups in the surfactant alkyl group; this interaction is absent when the head-group is perpendicular to the interface, as in dodecylpyridinium chloride. Therefore, FTIR and ^{1}H NMR data indicate that structure 5 of Fig. 2 is the most plausible conformation of the head-group in the micelle. As discussed below, this conclusion is also corroborated by Gibbs free energy of micellization.

Aggregation: Critical Micelle Concentration, Degree of Micelle Dissociation and Thermodynamic Parameters of Micellization

Examples of the dependence on [surfactant] of solution conductance and intensity of scattered light are shown in parts B to D of Fig. 4. Examples of calorimetric titration curves are shown in Fig. 7. In both figures, each graph shows a distinct break at the cmc, these are listed Table 1, along with available data for the corresponding $RAEtBzMe_2Cl$ and $RBzMe_2Cl$.

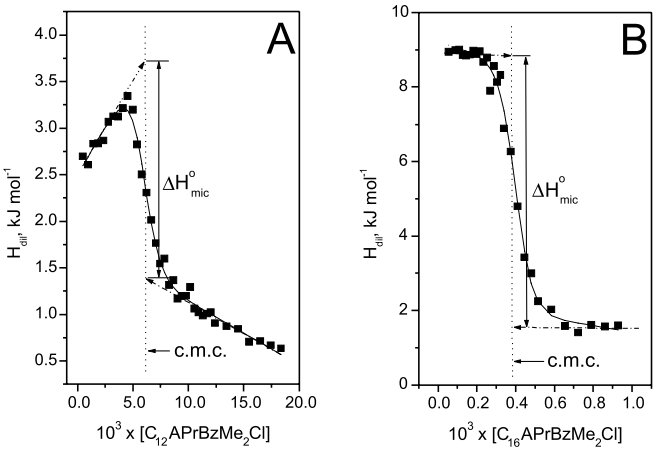

Fig. 7 Calorimetric titration curves at 25 °C, for $C_{12}APrBzMe_2Cl$ (**A**) and $C_{16}APrBzMe_2Cl$, (**B**). The *points* are experimental and the *solid line* was calculated by using Eq. 6

Regarding this Table, the following is relevant:

(i) There is an excellent agreement between the cmc values obtained by calorimetry and conductance, even for the C_{10} and C_{12} homologues, whose titration calorimetry plots clearly show non-ideal behavior. The dependence of the shape of these plots on the length of the surfactant hydrophobic tail has been discussed in terms of cmc, N_{agg} and α_{mic}. Small cmc and α_{mic}, and a large N_{agg} result in an intense heat pulse, exothermic or endothermic, detected by the calorimeter. A small cmc also means that the solutions in both sample cell and the injection syringe are essentially ideal (i.e., concentrations are equal to activities), so that the linear parts of the calorimetry titration plot, before and after the cmc, are independent of surfactant concentration, as shown for $C_{16}APrBzMe_2Cl$, Fig. 7B. A decrease in the length of the surfactant tail is accompanied with an increase of cmc and α_{mic}, and a decrease of N_{agg} [2, 3]. Consequently, the surfactant solution in the syringe and, with increasing injection number, in the sample cell, cannot be assumed to be ideal. This results in a concentration-dependent heat evolution and a smaller enthalpy variation at the cmc, as can be seen in Fig. 7A [45–47].

(ii) The IR-based cmc of $C_{10}APrBzMe_2Cl$ is 24.6×10^{-3} mol/L, i.e., ca. 10% higher than the cmc obtained by other techniques, in agreement with the fact that the tendency of surfactant aggregation in D_2O is larger than that in H_2O, because the former is a more structured solvent [48–51]. This is one of the few studies in which IR spectroscopy has been used to de-

termine cmc of surfactants [52–54], although IR and Raman spectroscopy have been fruitfully employed to study interactions (including hydrogen-bonding) within organized assemblies [55–58];

(iii) Value of α_{mic} is required in order to calculate Gibbs free energy of micelle formation, ΔG°_{mic}. Although Frahm's method is simple [30], it does not take into account the conductivity of the micelle (a "macro-ion") and leads, therefore, to α_{mic} higher than that calculated by Evans method, where this contribution is explicitly considered [31, 59]. Therefore, we use Evans equation-derived α_{mic} for calculation of ΔG°_{mic}, although both α_{mic} are listed in Table 1. We stress that α_{mic} calculated by Evans equation depends only slightly on N_{agg}. E.g., for $C_{14}APrBzMe_2Cl$ α_{mic} were found to be 0.22, 0.21 and 0.20 for $N_{agg} = 60$, 80 and 100, respectively;

(iv) For the same surfactant, $|\Delta H^{\circ}_{mic}|$ contributes less than $|T\Delta S^{\circ}_{mic}|$ to ΔG°_{mic}, i.e., micelle formation at 25 °C is entropy-driven. This can be understood in terms of the hydrophobic effect, namely micellization leads to a large gain in entropy because of the accompanied decrease in the hydrophobic surface area exposed to water. Additionally, the hydration of the head-group in the micelle is also readjusted due to monomer association and counter–ion condensation [1–3];

(v) Table 1 shows that increasing the length of the hydrophobic chain increases $T\Delta S^{\circ}_{mic}$ and decreases ΔH°_{mic} and ΔG°_{mic}. This is due to the accompanying increase in contribution of the hydrophobic hydration, due to an increase in N_{agg}, with a concomitant closer packing of the surfactant molecules in the micelle, and less water penetration between the head-groups. The accompanied increase in head-group repulsion is compensated by an increase in counter–ion binding [60];

(vi) The data listed in Table 1 show the following order: $|\Delta G^{\circ}_{mic}|_{RAPrBzMe_2Cl} > |\Delta G^{\circ}_{mic}|_{RAEtBzMe_2Cl} > |\Delta G_{mic}|_{RBzMe_2Cl}$. This order may be analyzed in terms of the contributions of the surfactant discrete segments, namely, the terminal CH_3 group of the hydrophobic chain, $\Delta G^{\circ}_{CH_3}$; the methylene groups of the alkyl chain, ($N_{CH_2}\Delta G^{\circ}_{CH_2}$) and the head-group, $\Delta G^{\circ}_{head\text{-}group}$, (Eq. 9) [1–3]:

$$\Delta G^{\circ}_{mic} = N_{CH_2} \cdot \Delta G^{\circ}_{CH_2} + \Delta G^{\circ}_{head\text{-}group} + \Delta G^{\circ}_{CH_3} \quad (9)$$

This equation predicts a linear correlation between ΔG°_{mic} and N_{CH_2}, where the intercept includes contributions from the terminal methyl plus the head-group. Since $\Delta G^{\circ}_{CH_3}$ is independent of the chain length of the surfactant, its contribution is constant in a homologous series. Therefore, the differences between the intercepts of the three surfactant series essentially reflect effects of the transfer of the head-groups from bulk solution to the micelle [1–3]. Equations similar to Eq. 9, and a similar line of reasoning apply to ΔH°_{mic}, and ΔS°_{mic}. The results (thermodynamic property/CH_2 and/or CH_3 plus head-group; and correlation coefficient) are listed in Table 2.

Table 2 shows the following:

(i) For the three homologue series, the contributions of the CH_2 groups of the alkyl chain to ΔG°_{mic} are similar, -3.5 ± 0.1 kJ/mol. This is expected because the transfer of these groups from water to the micellar core is practically independent of the structure of the head-group [1–3]. Other compounds show similar values: $\Delta G^{\circ}_{CH_2}$ for the transfer of alkanes from water to bulk hydrocarbon is -3.6 kJ mol^{-1} [61]; $\Delta G^{\circ}_{CH_2}$ are -3.3 and -3.1 kJ mol^{-1} for the aggregation in water of *n*-alkylmethylsulfoxides and *n*-alkyldimethylphosphine oxides, respectively [62, 63];

(ii) On the other hand, $\Delta G^{\circ}_{CH_3+head\text{-}group}$ for $RAPrBzMe_2Cl$ and $RAEtBzMe_2Cl$ are smaller, i.e., more favorable than the corresponding one of $RBzMe_2Cl$, as a consequence of smaller (i.e., less unfavorable) $\Delta H_{CH_3+head\text{-}group}$ and larger $\Delta S_{CH_3+head\text{-}group}$. As

Table 2 Contribution of the surfactant discrete segments, CH_2 and CH_3 + head-group to the thermodynamic parameters of micellization, at 25 °C

	ΔG°_{mic} (kJ mol^{-1})			ΔH°_{mic} (kJ mol^{-1})			$T\Delta S^{\circ}_{mic}$ (kJ mol^{-1})		
	CH_3 + head-group	CH_2	r [a]	CH_3 + head-group	CH_2	r [a]	CH_3 + head-group	CH_2	r [a]
$RAPrBzMe_2Cl$	−6.7 (±0.8)	−3.4 (±0.1)	0.9996	11.1 (±0.9)	−1.3 (±0.1)	0.9967	18 (±2)	2.1 (±0.1)	0.9953
$RAEtBzMe_2Cl$	−6.1 (±0.9)	−3.4 (±0.1)	0.9994	13.4 (±0.7)	−1.60 (±0.6)	0.9986	19.5 (±1)	1.8 (±0.1)	0.9947
$RBzMe_2Cl$	1.7 (±0.9)	−3.6 (±0.1)	0.9996	18 (±1)	−1.5 (±0.1)	0.9928	16 (±2)	2.1 (±0.2)	0.9914

[a] Correlation coefficient of the regression analysis

discussed above, the head-groups of $RAPrBzMe_2Cl$ and/or $RAEtBzMe_2Cl$ dehydrate on micelle formation because of inter-molecular hydrogen-bonding of the amide groups. This de-solvation is expected to be endothermic, because the enthalpy of transfer of quaternary ammonium ions from water to aqueous organic solvents (a model for interfacial water) is positive [64]. This (endothermic) process is compensated by an exothermic one (hydrogen-bonding between the amide groups), leading to energy compensation and the observed smaller contribution of $\Delta H_{CH_3+\text{head-group}}$. A couple of factors increase the degrees of freedom in micellar solutions of the amide group-carrying surfactants: release of water of hydration from the head-group due to amide group hydrogen-bonding; the higher flexibility of the tethers to which the benzyl groups of $RAPrBzMe_2Cl$ and/or $RAEtBzMe_2Cl$ are attached, relative to the relatively constrained benzyl group of $RBzMe_2Cl$;

(iii) Finally, a couple of important points emerge from examination of Gibbs free energies of the surfactant moieties: $|\Delta G^\circ_{CH_3+\text{head-group}}|$ of $RAPrBzMe_2Cl$ is slightly larger than that of $RAEtBzMe_2Cl$, due to the presence of an additional CH_2 group in the tether. The difference (0.6 kJ/mol) is small, however, because this group is still appreciably hydrated in the micelle, vide supra. Additionally, $(\Delta G^\circ_{CH_3+\text{head-group}})_{RAPrBzMe_2Cl} - (\Delta G_{CH_3+\text{head-group}})^\circ_{RAPrMe_3Cl}$ [65] measure the difference (at a constant spacer length, *n*-propyl) between the free energies of transfer of the benzyl group, relative to that of the methyl group, from bulk solution to the micellar pseudo-phase. This $\Delta\Delta G^\circ$ is relatively large, -4.9 kJ/mol, ca. $1.4 \times \Delta G^\circ_{CH_2}$, showing that the benzyl group in the micelle is present in a relatively hydrophobic environment, as depicted by structure 5 of Fig. 2.

Conclusions

A homologous series of benzyl (3-acylaminopropyl) dimethylammonium chloride surfactants has been synthesized and their aggregation in aqueous solution studied by ^1H NMR, FTIR (in D_2O), conductivity and calorimetry (in H_2O). The results indicate that the micelle/water interface lies close to the amide group, and that the benzyl moiety "folds back" toward the micellar interior. Thermodynamic parameters of micelle formation have been calculated and separated into contributions from the transfer of the discrete surfactant segments from bulk water to the micellar pseudo-phase. Micellization of surfactants that carry an amide head-group is more favorable than that of $RBzMe_2Cl$, due to direct or water-mediated hydrogen-bonding between these groups.

Acknowledgement We thank the State of São Paulo Research Foundation (FAPESP) for financial support and the Brazilian National Research Council (CNPq) for a research productivity fellowship to O.A. El Seoud, Prof. Watson Loh, UNICAMP for making the calorimeter available to us, and Dr. S. Shimizu for running the spectra of dodecylpyridinium chloride, Fig. 6.

References

1. Attwood D, Florence AT (1984) Surfactant Systems: Their Chemistry, Pharmacy, and Biology. Chapman and Hall, London
2. Rosen MJ (1989) Surfactants And Interfacial Phenomena. Wiley, New York
3. Hiemenz PC, Rajagopalan R (1997) Principles of Colloid and Surface Chemistry, 3rd ed. Marcel Dekker, New York
4. Bunton CA, Quina FH, Romsted LS (1991) Acc Chem Res 24:357
5. Bunton CA, Savelli G (1986) Adv Phys Org Chem 22:213
6. Bunton CA (1997) J Mol Liq 72:231
7. Birdi KS (1997) Handbook of Surface and Colloid Chemistry. CRC Press, Boca Raton, FL
8. Zana R (1997) Colloids Surfaces A 27:123
9. Okano LT, El Seoud OA, Halstead T (1997) Colloid Polym Sci 138:275
10. El Seoud OA, Blásko A, Bunton CA (1995) Ber Bunsenges Phys Chem 99:1214
11. Okano LT, Quina F, El Seoud OA (2000) Langmuir 16:3119
12. Blackmore ES, Tiddy GTJ (1988) J Chem Soc Faraday Trans 2 84:1115
13. Malliaris A, Paleos CM (1984) J Colloid Interface Sci 101:364
14. Burczyk B, Wilk KA (1990) Prog Colloid Polym Sci 82:249
15. Nowak JR, Pomianowski A, Szczena EN (1990) J Surface Sci Tecnol 6:287
16. Bazito RC, El Seoud OA, Barlow GK, Halstead TK (1997) Ber Bunsenges Phys Chem 101:1933
17. Kollman P (1993) Chem Rev 93:2395
18. Ludwig R, Reis O, Winter R, Weinhold F, Farrar TC (1998) J Phys Chem B 102:9312
19. Huelsekopf M, Ludwig R (2001) Mag Res Chem 39:127
20. Tsubone K, Rosen MJ (2001) J Colloid Interface Sci 244:394
21. Shimizu S, El Seoud OA (2003) Colloid Polym Sci 282:21
22. Shimizu S, El Seoud OA (2003) Langmuir 19:238
23. Shimizu S, Pires PAR, El Seoud OA (2003) Langmuir 19:9645
24. Shimizu S, Pires PAR, Fish H, Halstead TK, El Seoud OA (2003) Phys Chem Chem Phys 5:3489
25. Shimizu S, Pires PAR, Loh W, El Seoud OA (2004) Colloid Polym Sci 282:1026
26. Shimizu S, Pires PAR, El Seoud OA (2004) Langmuir 20:9551
27. Armarego WLF, Chai CLL (2003) Purification of Laboratory Chemicals. 5 ed. Elsevier, New York
28. Lide DR (ed) (1992) CRC Handbook of Chemistry and Physics. 73 ed. CRC Press, Boca Raton, FL

29. Carpena A, Aguiar J, Bernaola-Galván P, Ruiz CC (2002) Langmuir 18:6054
30. Frahm J, Diekmann S, Haase A (1980) Ber Bunsenges Phys Chem 84:566
31. Evans HC (1956) J Chem Soc 579
32. Király Z, Dékany I (2001) J Colloid Interface Sci 242:214
33. Solans C, Infante R, Azemar N, Wärnheim T (1989) Prog Colloid Polym Sci 79:70
34. Kunieda H, Nakamura K, Infante R, Solans C (1992) Adv Mat 4:291
35. Miyazawa T, Shimanouchi T, Mizushima S (1958) J Chem Phys 29:611
36. Chen CYS, Swenson CA (1969) J Phys Chem 73:2999
37. Eaton G, Symons MCR, Rastogi PP (1989) J Chem Soc Faraday Trans 1 85:3257
38. Symons MCR (1993) J Mol Structure 297:133
39. Schweitzer-Stenner R, Sieler G, Mirkin NG, Krimm S (1998) J Phys Chem A 102:118
40. Tada EB, Novaki LP, El Seoud OA (2001) Langmuir 17:652
41. Soldi V, Keiper J, Romsted LS, Cuccovia I, Chaimovich H (2000) Langmuir 16:59
42. Uemura J, Mantsch HH, Cameron DG (1981) J Colloid Interface Sci 83:558
43. Possidonio S, Siviero F, El Seoud AO (1999) J Phys Org Chem 12:325
44. Rózycka-Roszak B, Cierpicki T (1999) J Colloid Interface Sci 218:529
45. Nusselder JJH, Engberts JBFN (1992) J Colloid Interface Sci 148:353
46. Bijma K, Engberts JBFN, Blandamer MJ, Cullis PM, Last PM, Irlam KD, Soldi LG (1997) J Chem Soc Faraday Trans 93:1579
47. Blandamer MJ, Cullis PM, Engberts JBFN (1998) J Chem Soc Faraday Trans 94:2261
48. Mukerjee P, Kapauan P, Meyer HG (1966) J Phys Chem 70:783
49. Chou SI, Shah DO (1981) J Colloid Interface Sci 80:49
50. Candau S, Hirsch E, Zana R (1982) J Colloid Interface Sci 88:428
51. Elvingson C (1987) J Phys Chem 91:1455
52. Umemura J, Mantsch HH, Cameron DG (1981) J Colloid Interface Sci 83:558
53. Yang PW, Mantsch HH (1986) J Colloid Interface Sci 113:218
54. Etori F, Yamada H, Taga Y, Okabayashi K, Ohshima HK, O'Connor C (1997) J Vibrational Spect 14:133
55. Lafrance D, Marion D, Pézolet M (1990) Biochem 29:4592
56. Nilsson A, Holmgren A, Lindblom G (1994) Chem Phys Lipids 69:219
57. Domingo JC, Mora M, de Madariaga MA (1994) Chem Phys Lipids 69:229
58. Domingo JC, de Madariaga MA (1996) Chem Phys Lipids 84:147
59. Zana R (2002) J Colloid Interface Sci 246:182
60. Bijma K, Blandamer MJ, Engberts JBFN (1988) Langmuir 14:79
61. Nelson HD, de Ligny CL (1968) Rec Trav Chim 87:528
62. Clint JH, Walker T (1974) J Chem Soc Faraday Trans I 71:946
63. Lah J Pohar C, Vesnaver G (2000) J Phys Chem B 104:2522
64. Hefter G, Marcus Y, Waghorne WE (2002) Chem Rev 102:2773
65. $\Delta G^{\circ}_{CH_3+\text{head-group}}$ for the series 3-(acylaminopropyl) trimethylammonium chloride was found to be -1.8 kJ/mol, Pires PAR Ph D, thesis, the University of São Paulo, 2002
66. Mukerjee P, Mysels KJ (1971) Critical Micelle Concentrations of Aqueous Surfactant Systems, NSRDS: Washington